

Magnetization switching in nanoscale ferromagnetic grains: description by a kinetic Ising model

Howard L. Richards^{abc}, Scott W. Sides^{abc}, M. A. Novotny^b, and Per Arne Rikvold^{abc}

^a) *Center for Materials Research and Technology*, ^b) *Supercomputer Computations Research Institute*, and ^c) *Department of Physics, Florida State University, Tallahassee, Florida 32306-3016*

(December 23, 1994)

Abstract

The magnetic relaxation of ferromagnetic powders has been studied for many years, largely due to its importance to recording technologies. However, only recently have experiments been performed that resolve the magnetic state of individual sub-micron particles. Motivated by these experimental developments, we use droplet theory and Monte Carlo simulations to study the time and field dependence of some quantities that can be observed by magnetic force microscopy. Particular emphasis is placed on the effects of finite particle size. The qualitative agreement between experiments on switching and our simulations in individual single-domain ferromagnets suggests that the switching mechanism in such particles may involve local nucleation and subsequent growth of droplets of the stable phase.

Key words: nanoscale ferromagnets, magnetization switching, magnetic force microscopy, metastability

FSU-SCRI-94-131

PACS Number(s): 75.60.Jp, 75.70.-i, 64.60.My, 05.50.+q

Typeset using REVTeX

I. INTRODUCTION

Magnetic recording technologies are among the most important applications of permanent magnets today. A typical storage medium consists of fine magnetic particles suspended in an organic binder adhering to a polymer substrate. During the recording process, different regions of the medium are briefly exposed to strong magnetic fields, so that each grain is magnetized in the desired direction [1]. Each grain could thus in principle store one bit of data, so greater storage density could ideally be achieved by a medium containing many small grains than by one containing a few large grains. However, in order to serve as reliable storage devices, the grains must be capable of retaining their magnetizations for long periods of time in weaker, arbitrarily oriented ambient magnetic fields. Since experiments show the existence of a particle size at which the magnetizations are most stable (see, *e.g.*, Ref. [2]), there is a tradeoff between high storage capacity and long-term data integrity which must give rise to an optimum choice of grain size for any given material. During both recording and storage, the relationship between the magnetic field, the size of the grain, and the lifetime of the magnetization opposed to the applied magnetic field is therefore of great technological interest.

Fine ferromagnetic grains have been studied for many years, but until recently such particles could be studied experimentally only in powders (see, *e.g.*, Ref. [2]). This made it difficult to differentiate the statistical properties of single-grain switching from effects resulting from distributions in particle sizes, compositions, and local environments, or from interactions between grains. Magnetic force microscopy (MFM) (see, *e.g.*, Refs. [3–7]) and Lorentz microscopy (see, *e.g.*, Ref. [8]) now provide means for overcoming the difficulties in resolving the magnetic properties of individual single-domain particles.

The standard theory of magnetization reversal is a mean-field treatment due to Néel [9] and Brown [10,11]. In order to avoid an energy barrier due to exchange interactions between atomic moments with unlike orientations, Néel-Brown theory assumes uniform rotation of all the atomic moments in the system. The remaining barrier is caused by magnetic anisotropy [12], either intrinsic or shape-induced. Anisotropy makes it energetically favorable for each atomic moment to be aligned along one or more “easy” axes. Buckling, fanning, and curling are, like uniform rotation, theoretical relaxation processes with few degrees of freedom and global dynamics [1,13]. In all of the above approaches, the lifetime τ of the magnetization increases exponentially with the particle volume, L^d :

$$\tau \propto \exp(\beta L^d \Delta f) , \tag{1}$$

where d is the spatial dimension, $\beta^{-1} = k_B T$ is the temperature in units of energy, and Δf is the height of the free-energy density barrier to be crossed in the relaxation process.

However, for highly anisotropic materials there exists an alternative mode of relaxation with a typically much shorter lifetime. Small regions of the phase in which the magnetization is parallel to the applied magnetic field (the “stable” phase) are continuously created and destroyed by thermal fluctuations within the phase in which the magnetization is antiparallel to the field (the “metastable” phase). As long as such a region (henceforth referred to as a “droplet”) is sufficiently small, the short-ranged exchange interaction with the surrounding metastable phase imposes a net free-energy penalty, and the droplet will, with high probability, shrink and vanish. Should the droplet become larger than a critical size, however,

this penalty will be less than the benefit obtained from orienting parallel to the magnetic field, and the droplet will with a high probability grow further, eventually consuming the grain. The nature of the metastable decay thus depends on the relative sizes of the grain, the critical droplet, the average distance between droplets, and the lattice constant, as discussed in detail, *e.g.*, in Refs. [14–17].

At this point we wish to emphasize the difference between a droplet and a domain. Whereas they are both spatially continuous regions of uniform magnetization, a domain is an equilibrium feature whereas a droplet is a strictly non-equilibrium entity. A droplet may either grow or shrink, but it will not remain constant. All of the particles referred to in this paper are single-domain, which means that in equilibrium their magnetizations will be uniform, but as we shall see they may nevertheless decay through the nucleation and growth of droplets.

Because of its simplicity, the kinetic nearest-neighbor Ising model has been extensively studied as a prototype for metastable dynamics (see Ref. [17], and references cited therein). In particular, square- and cubic-lattice Ising systems with periodic boundary conditions have been used to study grain-size effects in ferroelectric switching [18,19]. A related one-dimensional model has been used to study magnetization reversal in elongated ferromagnetic particles [20–23]. In this article we use the kinetic Ising model to estimate the switching field, H_{sw} , at which magnetization reversal is thermally induced on experimental timescales for given temperatures and system sizes. (Figure 1 is a sketch of switching-field curves and the four regions of metastable decay for a typical metastable system with short-range interactions.) We also find explicit functional forms for what is actually observed in MFM experiments: the time- and field-dependent probability that a grain of given size remains unswitched.

The organization of the remainder of this paper is as follows. In Sec. II we describe the kinetic Ising model and the Monte Carlo methods we use to study metastable decay. A brief summary of the relevant results of droplet theory is given in Sec. III. We present our simulational estimates of quantities observable by magnetic force microscopy in Sec. IV. In Sec. V we conclude with a qualitative comparison with some recent experiments and discuss some of the implications of this work.

II. MODEL AND NUMERICAL METHODS

The model is defined by the Hamiltonian

$$\mathcal{H} = -J \sum_{\langle i,j \rangle} s_i s_j - HL^d m + DL^d m^2, \quad (2)$$

where $s_i = \pm 1$ is the z -component of the magnetization of the atom (spin) at site i , $J > 0$ is the ferromagnetic exchange interaction, H is the applied magnetic field times the single-spin magnetic moment. The sum $\sum_{\langle i,j \rangle}$ runs over all nearest-neighbor pairs on a square (generally hypercubic) lattice of side L . In this work we do not study the effects of grain boundaries, so periodic boundary conditions are imposed. The dimensionless system magnetization is given by

$$m = L^{-d} \sum_i s_i, \quad (3)$$

where the sum is over all L^d sites. The lattice constant is set to unity.

The last term in Eq. (2) allows for an approximate treatment of the magnetostatic energy. While a more detailed treatment using magnetic dipole-dipole interactions would be more physical, this approximation has a significant advantage in computational efficiency. For systems with periodic boundary conditions, the first and third terms of Eq. (2) are equal when the system size is given by

$$L_D \approx \frac{2\sigma_\infty(T)}{D}, \quad (4)$$

where $\sigma_\infty(T)$ is the surface tension along a primitive lattice vector in the limit $L \rightarrow \infty$. For the two-dimensional Ising model, $\sigma_\infty(T)$ is known exactly [24]. The length scale on which we would expect a transition from single-domain to multi-domain behavior is approximately L_D . In this work we set $D=0$, which reduces Eq. (2) to the standard Ising Hamiltonian and guarantees that the system will be single-domain at equilibrium for all system sizes. Studies of systems with $D>0$ will be reported elsewhere [25].

The selection of the Ising model is equivalent to requiring that the anisotropy constant be much greater than any other microscopic energy scale in the system. Since a large anisotropy is in fact required for magnetic materials used in magnetic recording media [1], this idealization may not be too unreasonable. Simplicity is our main reason for choosing periodic boundary conditions and a two-dimensional system, particularly since many equilibrium properties of the two-dimensional Ising model in zero field are known exactly [24] and since the kinetics of metastable decay has been extensively studied for this model. As a result, our model systems more closely resemble ultrathin magnetic films than magnetic grains. A more realistic simulation of three-dimensional grains is planned for later study, but we emphasize that we expect that droplet theory applies to almost any spin model with high anisotropy. Accordingly, equations are written in forms appropriate for arbitrary dimensionality d , even though simulations are only carried out for $d=2$.

The relaxation kinetics is simulated by the single-spin-flip Metropolis dynamic with updates at randomly chosen sites. This dynamic is realized by the original Metropolis algorithm [26] and the n -fold way algorithm [27]. (For a discussion on the equivalence of the dynamics of these algorithms, see Ref. [28].) The acceptance probability in the Metropolis algorithm for a proposed flip of the spin at site α from s_α to $-s_\alpha$ is defined as $W(s_\alpha \rightarrow -s_\alpha) = \min[1, \exp(-\beta\Delta E_\alpha)]$, where ΔE_α is the energy change due to the flip. The n -fold way algorithm is similar, but involves the tabulation of energy classes. First an energy class is chosen randomly with the appropriately weighted probability. A single site is then chosen from within that class with uniform probability and flipped with probability one. The number of Metropolis algorithm steps which would be required to achieve this change is chosen from a geometric probability distribution [28], and the time, measured in Monte Carlo steps per spin (MCSS), is incremented accordingly. The n -fold way algorithm is more efficient than the Metropolis algorithm at low temperatures, where the Metropolis algorithm requires many attempts before a change is made.

We study the relaxation of the dimensionless system magnetization starting from an initial state magnetized opposite to the applied field ($m(t=0) = +1, H < 0$). This approach has often been used in previous studies, *e.g.* in Refs. [16,29]. For the temperatures employed in this study, the equilibrium spontaneous magnetizations in zero field are close to unity,

with $0.95 < m_s < 1$. Since the applied field is negative (and generally small), the equilibrium magnetization is assumed to be approximately $-m_s$ and the metastable magnetization is assumed to be given by $m_{\text{ms}} \approx +m_s$. We use as an operational definition of the lifetime τ of the metastable phase the mean first-passage time to a cutoff magnetization $m=0$:

$$\tau = \langle t(m=0) \rangle . \quad (5)$$

It has been observed [16] that the qualitative results discussed below are not sensitive to the cutoff magnetization as long as it is sufficiently less than m_s . Our choice of $m=0$ as the cutoff facilitates comparison with MFM experiments, which are only capable of measuring the sign of the particle magnetization. Note that the *mean* first-passage time is generally not the same as the *median* first-passage time.

III. DROPLET THEORY

In this section we briefly review some elements of droplet theory. We concentrate specifically on the form of the lifetime within the four regions (shown in Fig. 1) of metastable decay for a typical metastable system with short-ranged interactions. As we will see below [Eqs. (8), (9), (14)], the exponential dependence of the metastable lifetime of a system with short-ranged interactions does not depend exponentially on the system volume, as is the case for a system with mean-field interactions [Eq. (1)]. For a more complete review, see Ref. [17].

At zero applied field, the system enjoys true coexistence between two degenerate equilibrium phases with magnetizations $m \approx \pm m_s \approx \pm 1$. This leads to the identification of a ‘‘Coexistence’’ (CE) region [15,16] within which the applied field is so weak that metastable decay proceeds only through a single, system-spanning subcritical droplet. The field limiting the CE region is called the ‘‘Thermodynamic Spinodal’’ (H_{ThSp}) [15,16]. The radius of a critical droplet, given by [17]

$$R_c = \frac{(d-1)\sigma_\infty(T)}{2|H|m_s} , \quad (6)$$

provides a criterion for estimating the crossover to decay by a single droplet. We estimate $|H_{\text{ThSp}}|$ by setting $2R_c = (L-1)$, which yields

$$|H_{\text{ThSp}}| \approx \frac{(d-1)\sigma_\infty(T)}{(L-1)m_s} . \quad (7)$$

For a short-range-force system in the CE region the free-energy barrier that must be crossed comes mostly from the creation of an interface at intermediate system magnetizations. The resulting form for the lifetime for systems with periodic boundary conditions is [30–32]

$$\tau(L, H, T) \approx A(T) \exp \left\{ 2\beta\sigma_L(T)L^{d-1} [1 + O(HL)] \right\} , \quad (8)$$

where $A(T)$ is a non-universal prefactor and $\sigma_L(T)$ is the L -dependent surface tension along a primitive lattice vector. Any power-law prefactors in Eq. (8) are absorbed into this definition

of $\sigma_L(T)$ as $O[(\ln L)/L]$ terms. The $O(HL)$ term comes from bulk contributions to the free energy.

The region of fields just stronger than H_{ThSp} is called the ‘‘Single-Droplet’’ (SD) region [15,16]. In this region the first critical droplet to nucleate almost always grows to fill the system before any other droplet has a chance to nucleate. The lifetime in the SD region is given in terms of the nucleation rate per unit volume I by [17]

$$\tau(L, H, T) \approx [L^d I(T, H)]^{-1} . \quad (9)$$

The nucleation rate $I(T, H)$ is given by

$$I(T, H) \approx B(T)|H|^K \exp \left\{ -|H|^{1-d} [\Xi_0(T) + \Xi_1(T)H^2] \right\} , \quad (10)$$

where $B(T)$ is a non-universal prefactor, and K is believed to be 3 for the two-dimensional Ising model and $-1/3$ for the three-dimensional Ising model [16]. Here $\Xi_0(T)$ is given by [17]

$$\Xi_0(T) \equiv \beta\Omega [\sigma_\infty(T)]^d \left[\frac{d-1}{2m_s} \right]^{d-1} , \quad (11)$$

where Ω is a shape- and dimension-dependent constant such that the volume of a droplet is given in terms of its radius by $V = \Omega R^d$. For the two-dimensional Ising model, Ω is exactly known [17]. We determine Ξ_1 from a numerical fit.

In both the CE and SD regions, switching is abrupt, with a negligible amount of time being spent in configurations with magnetizations other than $\pm m_s$. This phenomenon, in which the entire system behaves as though it were a single magnetic moment, is known as superparamagnetism [12,33]. Switching is a Poisson process in both the CE and SD regions, so the probability $P(m > 0)$ that the magnetization is greater than zero decays exponentially with time, and the median switching time is larger than the mean switching time by a factor of $\ln 2$. The standard deviation of the switching time for an individual grain is approximately equal to the mean switching time, τ . Because of the random nature of switching in the CE and SD regions, their union has been called the ‘‘Stochastic Region’’ [15,16].

Still stronger fields, by contrast, lead to decay through many weakly interacting droplets in the manner described by Kolmogorov [34], Johnson and Mehl [35], and Avrami [36–38]. Such decay is ‘‘deterministic’’ in the sense that the standard deviation of the switching time is much less than its mean (see the Appendix). The crossover between the SD region and the multi-droplet (MD) region has been called the ‘‘Dynamic Spinodal’’ (Dsp) [15,16]. Since the standard deviation of the lifetime is equal to its mean in the Stochastic region, we estimate this crossover by the field $H_{1/2}$ at which

$$\sqrt{\langle t^2(m=0) \rangle - \tau^2} = \frac{\tau}{2} . \quad (12)$$

For *asymptotically* large L , H_{Dsp} tends to zero as [16]

$$H_{\text{Dsp}} \sim \left[\frac{\Xi_0(T)}{(d+1) \ln L} \right]^{1/(d-1)} \left\{ 1 + \frac{K-1}{d^2-1} \left[\frac{\ln(\ln L)}{\ln L} \right] + \left[\ln \left(\frac{\nu}{B} \right) - \frac{K-1}{d-1} \ln \left(\frac{\Xi_0}{d+1} \right) + \frac{\ln(2\Omega)}{d} \right] \left(\frac{1}{(d+1) \ln L} \right) \right\} ; \quad (13)$$

however, extremely large system sizes may be required before this scaling form is observed.

Within the MD region the lifetime is given by [17]

$$\tau(L, H, T) \approx \left[\frac{\Omega v^d}{(d+1) \ln 2} I(T, H) \right]^{-\frac{1}{d+1}}, \quad (14)$$

where $I(T, H)$ is given by Eq. (10). Here v is the (nonuniversal) temperature-dependent radial growth velocity of a droplet, which under an Allen-Cahn approximation [39–41] is proportional to the applied field in the limit of large droplets:

$$v \approx \nu |H|. \quad (15)$$

At a sufficiently high field, nucleation becomes much faster than growth and the droplet picture breaks down. The crossover to this “Strong-Field” region (SF) has been called the “Mean-Field Spinodal” (MFSp) [15,16]. A conservative estimate for this crossover field is obtained by setting $2R_c = 1$:

$$|H_{\text{MFSp}}| \approx \frac{(d-1)\sigma_\infty(T)}{m_s}. \quad (16)$$

IV. MONTE CARLO SIMULATIONS OF MFM OBSERVABLES

The droplet-theory concepts of Sec. III provide a framework for the calculation of a number of observable quantities. In this section we discuss calculations of MFM observables from Monte Carlo simulations of the two-dimensional kinetic Ising model as discussed in Sec. II.

The mean first-passage time τ to $m = 0$ can be found at a fixed magnetic field directly from Monte Carlo simulations. Finding the magnetic field corresponding to a given lifetime requires an indirect approach. From four fields chosen such that $\tau(L, H, T) \approx t$ at fixed system size L and temperature T , we use weighted linear regression to estimate the switching field $H_{\text{sw}}(L; t, T)$ such that $\tau(L, H_{\text{sw}}, T) = t$. The results, which are shown in Fig. 2 for three different temperatures and a range of system sizes and waiting times, are qualitatively similar to experimental measurements of the same quantity made on powders (see, *e.g.*, Ref. [2]) and on single-domain particles [4]. As Fig. 2 illustrates, the maximum value of $H_{\text{sw}}(L; t, T)$ occurs within the SD region. The asymptotically nonzero value of $H_{\text{sw}}(L; t, T)$ in the MD region is not observed in actual experiments, perhaps because defects and impurities lead to heterogenous nucleation in large grains. Lastly, a comparison of parts (a), (b), and (c) of Fig. 2 shows the striking temperature dependence of H_{sw} for a fixed waiting time.

From MFM experiments one does not measure magnetization, but rather detects the orientation of the magnetic poles, *i.e.*, the sign of m . An experimentally measurable quantity that can be used to determine the decay mode is therefore the probability that the magnetization is greater than zero, $P(m > 0)$, as a function of field at fixed waiting time or as a function of waiting time at fixed field. The particular functional form of P which is predicted by droplet theory depends upon the region (CE, SD, MD, or SF) in which $P(m > 0) \approx 1/2$.

In the CE region, switching is a Poisson process and the decay of $\langle m(t) \rangle$ has an exponential form. However, recrossing (returning to an $m > 0$ phase from an $m \leq 0$ phase) is

important because the energy difference between the “stable” and “metastable” phases is so small. This is most easily seen at $H=0$, where the two phases coexist and

$$P(m > 0) = [\exp(-2t/\tau) + 1]/2 . \quad (17)$$

The factor of two in the exponential comes from the fact that τ is the mean first-passage time to $m=0$, not to $m=-m_s$. Figure 3(a) shows MC estimates of $P(m > 0)$ as a function of time, and Fig. 4(a) shows MC estimates of $P(m > 0)$ as a function of field in the CE region.

Because the energy difference between the stable and metastable phases is large in the SD region, the probability of return to $m > 0$ from $m \leq 0$ is negligible. As a result, $P(m > 0)$ decays exponentially in time, and we specifically obtain

$$P(m > 0) = \exp \left[\frac{-t}{\tau(L, H, T)} \right] , \quad (18)$$

where $\tau(L, H, T)$ is given by Eqs. (9) and (10). Note that $P(m > 0)|_{t=\tau} = 1/e \neq 1/2$ because the mean of an exponential distribution is not the same as its median. In Fig. 3(b), Monte Carlo estimates of $P(m > 0)$ as a function of t at fixed H, T , and L are seen to agree well with an exponential time decay. Figure 4(b) shows Monte Carlo estimates of P as a function of H at fixed t, T , and L together with fits based on Eqs. (9), (10), and (18). The fit shown in Fig. 4(b) comes from a least-squares fit used to determine $B(T)$ and $\Xi_1(T)$ in Eq. (10) [42]. The fit is seen to agree excellently with the MC data.

The form of $P(m > 0)$ in the MD region is somewhat more complicated and is derived in the Appendix. Both the switching field and the lifetime have asymptotically Gaussian probability distributions. Expanding in time around $t=\tau$ we find

$$P(m > 0)|_H \approx \frac{1}{2} \left[1 + \operatorname{erf} \left(\frac{t - \tau}{L^{-d/2} \Delta_t} \right) \right] , \quad (19)$$

where τ is given by Eq. (14) with $H = H_{\text{sw}}$. Here Δ_t is given by

$$\Delta_t = \frac{(\nu |H_{\text{sw}}|)^{d/2} \tau^{(d+2)/2}}{(d+1) \psi_d} \quad (20)$$

and ψ_d is given in Table I. Likewise, an expansion in field around H_{sw} yields

$$P(m > 0)|_t \approx \frac{1}{2} \left[1 + \operatorname{erf} \left(\frac{H - H_{\text{sw}}}{L^{-d/2} \Delta_H} \right) \right] , \quad (21)$$

where

$$\Delta_H = (\tau \nu |H_{\text{sw}}|)^{d/2} \left\{ \frac{d+K}{|H_{\text{sw}}|} - |H_{\text{sw}}|^{-d} [(1-d) \Xi_0 + (3-d) \Xi_1 H_{\text{sw}}^2] \right\}^{-1} \psi_d^{-1} . \quad (22)$$

Here H_{sw} is the switching field corresponding to the time τ .

Valuable dynamical information can be found by fitting the MC data to Eqs. (19) and (21). From the fit to Eq. (19) shown in Fig. 3(c) we can find ν and τ at fixed H directly (Tab. II). In order to find ν from Eq. (21) it is first necessary to find Ξ_1 . We therefore fit

MC estimates of τ to Eqs. (10) and (14) to find B and Ξ_1 [43]. The resulting estimates for ν are consistent with the estimate from Eq. (19) (Tab. II). Note that for the range of fields shown in Fig. 4(c) the radial growth velocity is less than one lattice constant per MCSS, which is to be expected from a single-spin-flip dynamic such as we are using.

Knowledge of B , Ξ_1 , and ν also allows us to find an alternative estimate for the Dynamic Spinodal. The crossover between the SD and MD regions can be expected to occur where the mean waiting time for a droplet to nucleate is approximately equal to the time required for a nucleated droplet to grow to volume $L^d/2$. This leads us to

$$\left[L^d I(T, H)\right]^{-1} = (\nu|H|)^{-1} \left[(2\Omega)^{-1/d} L - R_c\right], \quad (23)$$

where R_c is the critical droplet radius given in Eq. (6). As shown by the dot-dot-dashed curve in Fig. 2(c), this estimate for the Dynamic Spinodal is qualitatively similar to the estimate given by Eq. (12) but is quantitatively different. This is not surprising, since the Dynamic Spinodal is a crossover region, and its precise location depends on the manner in which it is defined.

It is also possible to approximately count the number of critical droplets which nucleate during the lifetime of the metastable state. By multiplying the nucleation rate by the volume of the system and the lifetime [from Eq. (14)] we find

$$N_{\text{drop}} = L^d I(T, H) \left[\frac{\Omega \nu^d |H|^d}{(d+1) \ln 2} I(T, H) \right]^{-\frac{1}{d+1}}. \quad (24)$$

Figure 5 shows a typical realization of magnetization reversal in the MD region. From Eq. (6), at $T=0.8T_c$ and $H=-0.2J$ a critical droplet consists of approximately 48 overturned spins. According to Eq. (24), approximately 18 critical droplets should have nucleated in the system shown in Fig. 5 by the time $m=0$, which is in rough agreement with visual inspection of the figure. However, it is difficult to confirm this number with precision directly from the “snapshots” since i) the droplets may partially or completely overlap, ii) the droplets may have irregular shapes, iii) there are many subcritical droplets, and iv) only a few times are displayed.

As a cautionary note, we analyze data taken in the SF region using equations appropriate for the MD region. As Fig. 3(d) and Fig. 4(d) show, Eqs. (19) and (21) can be fitted to the MC data for $P(m>0)$ quite well. This is because in the deterministic region, the observed magnetization is essentially an average over the magnetizations of regions too distant to be correlated, so that by the Central Limit Theorem it tends to a Gaussian distribution as $L \rightarrow \infty$. Interestingly, both the value of ν obtained from the fit in Fig. 3(d) [$\nu=0.875(9)$] and the value from the fit in Fig. 4(d) [$\nu=0.82(2)$] are in fairly good agreement with the values derived in the MD region (Tab. II). However, the resulting radial growth velocities ($v \approx 3$ lattice constants per MCSS) are too large to be meaningful in a single-spin-flip dynamic. Furthermore, whereas Eq. (14) gives a good fit for τ in the MD region, it fails when applied to the entire deterministic region. Since it will be extremely difficult to determine whether the radial growth velocity is reasonable in experimental systems (due to uncertainty about the appropriate classical dynamic and attempt frequency), droplet theory should be applied only if both Eq. (14) correctly gives the field-dependence of the lifetime and $H < H_{\text{MFSP}}$.

V. DISCUSSION

Due to the importance of magnetic recording technologies in modern society, magnetic relaxation has been a subject of study for many years. An early mean-field theory for this process was presented by Néel [9] and Brown [10,11] almost fifty years ago, and the most popular current models remain mean-field [1,13]. This is understandable, since mean-field models are much simpler to solve than models with local dynamics that describe spatial fluctuations. However, a great deal of research has been conducted on non-mean-field descriptions of metastability, particularly for the simple prototype model of anisotropic magnetism, the Ising model. These studies make it possible to obtain a more detailed understanding of magnetic relaxation.

In this paper we have discussed the magnetic relaxation of single-domain magnetic particles in terms of the droplet theory of metastable decay. We have performed Monte Carlo simulations of the metastable decay of two-dimensional Ising systems, and shown that these simulations yield switching fields which vary with system size in a manner which is qualitatively similar to experiments conducted on real single-domain particles (Fig. 2). We have also used droplet theory to determine the analytical forms of the probability that the magnetization remains unswitched, and fitted these forms to our simulation data (Figs. 3 and 4). The methods used in carrying out these fits are appropriate for use with experimental data obtained from magnetic force microscopy.

Because of their two-dimensional nature, the systems we have simulated with MC actually serve better as models of ultrathin islands of magnetic material on a nonmagnetic substrate. (For a review of experimental observations of the magnetic states of ultrathin films, see Ref. [44].) The symmetry of our lattice and the use of Ising spins require the modeled material to have strong perpendicular anisotropy. Several such ultrathin films have been observed to have critical exponents consistent with the universality class of the two-dimensional Ising model (see *e.g.* Refs. [45–49]). It would be interesting to compare microscopic observations of magnetization reversal in these films with the kinetic Ising model described in this paper.

Because films have macroscopic lateral extents ($L \gg 1$), it is difficult to study any kind of finite-size effects in them. One way to impose a finite size to a film is to grow it epitaxially on a stepped surface vicinal to a simple facet so that the width of the step is of a microscopically moderate size (see *e.g.* Ref. [50] and references therein). Of particular interest is Fe(110) on W(110), since at submonolayer coverages the iron can be grown on step edges of the tungsten surface and since the resulting film belongs to the two-dimensional Ising model universality class [49]. For such semi-infinite systems Monte Carlo simulations such as have been carried out here are not possible. Sophisticated techniques in statistical mechanics involving transfer matrices have, however, been successfully applied to the two-dimensional Ising model in strip geometry [51,52] and to a quasi-one-dimensional Ising model [53]. In both cases, it was found that concepts from droplet theory are useful in describing the metastable decay.

It is important to understand the relaxation process in the multi-droplet region clearly, both because it is relevant to ultra-thin films and some single-domain particles and because of controversies which have arisen over the mechanism of magnetic relaxation [54]. First of all, we re-emphasize that droplets are distinct from domains in that they are non-equilibrium

entities. Second, our model systems do not include defects or impurities to serve as nuclei. In fact, by using periodic boundary conditions and the initial condition $m(0) = +1$, all sites are completely equivalent; this symmetry is spontaneously broken only by local thermal excitations. Third, our model system is not a spin glass even though the time-dependence of the magnetization may occur as a stretched-exponential function [Eqs. (A1) and (A2)]. Finally, the simulations we have carried out are for an individual particle with a well-defined orientation. This distinguishes it from some treatments of magnetic viscosity, *e.g.* Ref. [55]. This last point also emphasizes the importance of experiments like MFM which resolve the magnetic state of isolated individual ferromagnetic particles.

ACKNOWLEDGMENTS

The authors wish to thank S. von Molnar, D. M. Lind, J. W. Harrell, W. D. Doyle, and B. M. Gorman for useful discussions and for comments on the manuscript. This research was supported in part by the Florida State University Center for Materials Research and Technology, by the FSU Supercomputer Computations Research Institute, which is partially funded by the U. S. Department of Energy through Contract No. DE-FC05-85ER25000, and by the National Science Foundation through Grants No. DMR-9013107 and DMR-9315969.

APPENDIX:

Avrami's Law [34–38] gives the volume fraction of the metastable state (or equivalently, the magnetization) for systems in which droplets nucleate with a rate (per unit volume) I and grow without interacting, although they may overlap. The time-dependent system magnetization $\langle m(t) \rangle$ is given by [34–38]

$$\langle m(t) \rangle \approx m_s [2\langle \phi(t) \rangle - 1] , \quad (\text{A1})$$

where

$$\langle \phi(t) \rangle = \exp \left[-\ln 2 \left(\frac{t}{\tau} \right)^{d+1} \right] \quad (\text{A2})$$

is the volume fraction of the metastable phase and τ is given by Eq. (14). The factor $\ln 2$ is necessary to fulfill the requirement $m(\tau) = 0$, in agreement with the definition of τ as the first-passage time to $m = 0$ [Eq. (5)].

The nucleation of droplets is random in both space and time, so only the mean magnetization is given by Eq. (A1). The variance in the magnetization is related to the two-point correlation function, which has been calculated by Sekimoto [56] for circular and spherical droplets. Specifically, if the system is described by a two-valued field $u(\mathbf{r}, t)$ where

$$u(\mathbf{r}, t) = \begin{cases} 1 & \text{if the position } \mathbf{r} \text{ is within the metastable phase at time } t, \\ 0 & \text{otherwise,} \end{cases} \quad (\text{A3})$$

then the connected two-point correlation function is given by [56]

$$\begin{aligned} \langle u(\mathbf{x}, t)u(\mathbf{x} + \mathbf{r}, t) \rangle - \langle u(\mathbf{x}, t) \rangle^2 \\ = \begin{cases} \langle u(\mathbf{0}, t) \rangle^2 \left\{ \exp \left[I v^d t^{d+1} \Psi_d(r/2vt) \right] - 1 \right\}, & r < 2vt \\ 0, & r > 2vt \end{cases} \end{aligned} \quad (\text{A4})$$

where $r \equiv |\mathbf{r}|$, and [56]

$$\Psi_2(y) = \frac{2}{3} \left[\cos^{-1} y - 2y\sqrt{1-y^2} + y^3 \ln \left(\frac{1 + \sqrt{1-y^2}}{y} \right) \right], \quad (\text{A5a})$$

$$\Psi_3(y) = \frac{\pi}{3} (1-y)^3 (1+y). \quad (\text{A5b})$$

Since $\langle \phi(t) \rangle$ is simply an average over $u(\mathbf{r}, t)$, with

$$\langle \phi(t) \rangle = L^{-d} \int \langle u(\mathbf{r}, t) \rangle d\mathbf{r}, \quad (\text{A6})$$

the variance of the magnetization is given by

$$\text{Var}[m(t)] \approx 4m_s^2 L^{-d} \int \left[\langle u(\mathbf{0}, t)u(\mathbf{r}, t) \rangle - \langle u(\mathbf{0}, t) \rangle^2 \right] d\mathbf{r} \quad (\text{A7a})$$

$$\begin{aligned} &= 4m_s^2 d\Omega L^{-d} \int_0^{2vt} r^{d-1} \left[\langle u(\mathbf{0}, t)u(\mathbf{r}, t) \rangle - \langle u(\mathbf{0}, t) \rangle^2 \right] dr \\ &= 4m_s^2 d\Omega \langle \phi(t) \rangle^2 \left(\frac{2vt}{L} \right)^d \int_0^1 y^{d-1} \left\{ \exp \left[I v^d t^{d+1} \Psi_d(y) \right] - 1 \right\} dy \\ &= 4m_s^2 d\Omega \langle \phi(t) \rangle^2 \left(\frac{2vt}{L} \right)^d \\ &\quad \times \left\{ -\frac{1}{d} + \int_0^1 y^{d-1} \exp \left[\frac{(d+1) \ln 2}{\Omega} \left(\frac{t}{\tau} \right)^{d+1} \Psi_d(y) \right] dy \right\}. \end{aligned} \quad (\text{A7b})$$

The total system magnetization at time t is thus seen to be essentially an average over on the order of $(L/2vt)^d$ independent samples. As a result of the Central Limit Theorem, for sufficiently large L , the distribution in magnetization is well approximated by a Gaussian distribution. Introducing the standard deviation in the magnetization,

$$\sigma(t) \equiv \sqrt{\text{Var}[m(t)]} \quad (\text{A8})$$

(not to be confused with the surface tension σ_L which is discussed in the text), it is easy to calculate the probability that the magnetization is greater than zero:

$$\begin{aligned} P(m > 0) &\approx \int_0^\infty \frac{1}{\sigma(t)\sqrt{2\pi}} \exp \left\{ -\frac{[\mu - \langle m(t) \rangle]^2}{2\sigma^2(t)} \right\} d\mu \\ &= \frac{1}{2} \left[1 + \text{erf} \left(\frac{\langle m(t) \rangle}{\sigma(t)\sqrt{2}} \right) \right]. \end{aligned} \quad (\text{A9})$$

This probability will differ from zero or one only if $\langle m(t) \rangle / \sigma(t) \approx 0$. Making a Taylor expansion in time for $\langle m(t) \rangle / \sigma(t)$ we find

$$P(m > 0)|_H \approx \frac{1}{2} \left[1 + \text{erf} \left(\frac{t - \tau}{L^{-d/2} \Delta_t} \right) \right], \quad (\text{A10})$$

where Δ_t is given by

$$\Delta_t = \frac{(\nu|H_{\text{sw}}|)^{d/2}\tau^{(d+2)/2}}{(d+1)\psi_d} \quad (\text{A11})$$

where ν is given by Eq. (15), τ is given by Eq. (14) with $H = H_{\text{sw}}$, and ψ_d is the constant given by

$$\psi_d \equiv \ln 2 \left(2^d d \Omega \left\{ -\frac{1}{d} + \int_0^1 y^{d-1} \exp[(d+1) \ln 2 \Psi_d(y)/\Omega] dy \right\} \right)^{-1/2}. \quad (\text{A12})$$

Table I lists numerical evaluations of ψ_d . Likewise, a Taylor expansion of $\langle m(t) \rangle / \sigma(t)$ in field yields

$$P(m > 0)|_t \approx \frac{1}{2} \left[1 + \operatorname{erf} \left(\frac{H - H_{\text{sw}}}{L^{-d/2} \Delta_H} \right) \right], \quad (\text{A13})$$

where

$$\Delta_H = (\tau \nu |H_{\text{sw}}|)^{d/2} \left\{ \frac{d+K}{|H_{\text{sw}}|} - |H_{\text{sw}}|^{-d} [(1-d)\Xi_0 + (3-d)\Xi_1 H_{\text{sw}}^2] \right\}^{-1} \psi_d^{-1}. \quad (\text{A14})$$

Here H_{sw} is the switching field corresponding to the time τ .

REFERENCES

- [1] E. Köster and T. C. Arnoldussen, in *Magnetic Recording*, edited by C. D. Mee and E. D. Daniel (McGraw-Hill, New York, 1987), Vol. 1, p. 98.
- [2] E. F. Kneller and F. E. Luborsky, *J. Appl. Phys.* **34**, 656 (1963).
- [3] Y. Martin and H. K. Wickramasinghe, *Appl. Phys. Lett.* **50**, 1455 (1987).
- [4] T. Chang, J.-G. Zhu, and J. H. Judy, *J. Appl. Phys.* **73**, 6716 (1993).
- [5] M. Lederman, G. A. Gibson, and S. Schultz, *J. Appl. Phys.* **73**, 6961 (1993).
- [6] M. Lederman, D. R. Fredkin, R. O'Barr, and S. Schultz, *J. Appl. Phys.* **75**, 6217 (1994).
- [7] M. Lederman, S. Schultz, and M. Ozaki, *Phys. Rev. Lett.* **73**, 1986 (1994).
- [8] C. Salling, S. Schultz, I. McFadyen, and M. Ozaki, *IEEE Trans. Magn.* **27**, 5184 (1991).
- [9] L. Néel, *Ann. Géophys.* **5**, 99 (1949).
- [10] W. F. Brown, *J. Appl. Phys.* **30**, 130S (1959).
- [11] W. F. Brown, *Phys. Rev.* **130**, 1677 (1963).
- [12] I. S. Jacobs and C. P. Bean, in *Magnetism*, edited by G. T. Rado and H. Suhl (Academic, New York, 1963), Vol. 3, p. 271.
- [13] E. Kneller, in *Magnetism and Metallurgy*, edited by A. E. Berkowitz and E. Kneller (Academic, New York, 1969), Vol. 1.
- [14] H. Orihara and Y. Ishibashi, *J. Phys. Soc. Jpn.* **61**, 1919 (1992).
- [15] H. Tomita and S. Miyashita, *Phys. Rev. B* **46**, 8886 (1992).
- [16] P. A. Rikvold, H. Tomita, S. Miyashita, and S. W. Sides, *Phys. Rev. E* **49**, 5080 (1994).
- [17] P. A. Rikvold and B. M. Gorman, in *Annual Reviews of Computational Physics I*, edited by D. Stauffer (World Scientific, Singapore, 1994), p. 149.
- [18] H. M. Duiker and P. D. Beale, *Phys. Rev. B* **41**, 490 (1990).
- [19] P. D. Beale, *Integrated Ferroelectrics* **4**, 107 (1994).
- [20] H. B. Braun, *Phys. Rev. Lett.* **71**, 3557 (1993).
- [21] H. B. Braun, *J. Appl. Phys.* **75**, 4609 (1994).
- [22] H. B. Braun, *Phys. Rev. B* **50**, 16485 (1994).
- [23] H. B. Braun, *Phys. Rev. B* **50**, 16501 (1994).
- [24] L. Onsager, *Phys. Rev.* **65**, 117 (1944).
- [25] H. L. Richards, M. A. Novotny, and P. A. Rikvold, (in preparation) (unpublished).
- [26] N. Metropolis *et al.*, *J. Chem. Phys.* **21**, 1087 (1953).
- [27] A. B. Bortz, M. H. Kalos, and J. L. Lebowitz, *J. Comp. Phys.* **17**, 10 (1975).
- [28] M. A. Novotny, *Computers in Physics* (1995), (in press).
- [29] D. Stauffer, *Int. J. Mod. Phys. C* **3**, 1059 (1992).
- [30] K. Binder, *Z. Phys. B* **43**, 119 (1981).
- [31] K. Binder, *Phys. Rev. A* **25**, 1699 (1982).
- [32] B. Berg, U. Hansmann, and T. Neuhaus, *Z. Phys. B* **90**, 229 (1993).
- [33] C. P. Bean and J. D. Livingston, *J. Appl. Phys.* **30**, 120S (1959).
- [34] A. N. Kolmogorov, *Bull. Acad. Sci. USSR, Mat. Ser.* **1**, 355 (1937).
- [35] W. A. Johnson and P. A. Mehl, *Trans. A.I.M.M.E.* **135**, 365 (1939).
- [36] M. Avrami, *J. Chem. Phys.* **7**, 1103 (1939).
- [37] M. Avrami, *J. Chem. Phys.* **8**, 212 (1940).
- [38] M. Avrami, *J. Chem. Phys.* **9**, 177 (1941).
- [39] I. M. Lifshitz, *Sov. Phys. JETP* **15**, 939 (1962).
- [40] S. K. Chan, *J. Chem. Phys.* **67**, 5755 (1977).

- [41] S. M. Allen and J. W. Cahn, *Acta Metall.* **27**, 1085 (1979).
- [42] For $L = 10$ and $T = 0.8T_c$, the fit yields $B = 0.20(1)J^{-K}/\text{MCSS}$ and $\Xi_1 = 9.1(3)J^{d-3}$.
- [43] For $L = 30$ and $T = 0.8T_c$, the fits yield $B = 0.018(2)J^{-K}/\text{MCSS}$ and $\Xi_1 = 2.0(2)J^{d-3}$.
For $L = 100$ and $T = 0.8T_c$, the fits yield $B = 0.028(4)J^{-K}/\text{MCSS}$ and $\Xi_1 = 3.0(3)J^{d-3}$.
The discrepancy between these results and those from the single-droplet region [42] are probably due to finite-size effects in the small systems.
- [44] R. Allenspach, *J. Magn. Magn. Mater.* **129**, 160 (1994).
- [45] Z. Q. Qiu, J. Pearson, and S. D. Bader, *Phys. Rev. Lett.* **67**, 1646 (1991).
- [46] J. Kohlhepp, H. J. Elmers, S. Cordes, and U. Gradmann, *Phys. Rev. B* **45**, 12287 (1992).
- [47] Y. Li and K. Baberschke, *Phys. Rev. Lett.* **68**, 1208 (1992).
- [48] Z. Q. Qiu, J. Pearson, and S. D. Bader, *Phys. Rev. B* **49**, 8797 (1994).
- [49] H. J. Elmers *et al.*, *Phys. Rev. Lett.* **73**, 898 (1994).
- [50] D. S. Chuang, C. A. Ballentine, and R. C. O'Handley, *Phys. Rev. B* **49**, 15084 (1994).
- [51] C. C. A. Günther, P. A. Rikvold, and M. A. Novotny, *Phys. Rev. Lett.* **71**, 3898 (1993).
- [52] C. C. A. Günther, P. A. Rikvold, and M. A. Novotny, *Physica A*, (in press).
- [53] B. M. Gorman, P. A. Rikvold, and M. A. Novotny, *Phys. Rev. E* **49**, 2711 (1994).
- [54] A. Aharoni, in *Magnetic Properties of Fine Particles*, edited by J. L. Dormann and D. Fiorani (North Holland, New York, 1992).
- [55] R. W. Chantrell and K. O'Grady, in *Magnetic Properties of Fine Particles*, edited by J. L. Dormann and D. Fiorani (North Holland, New York, 1992).
- [56] K. Sekimoto, *Physica A* **135**, 328 (1986).

FIGURES

FIG. 1. The relationship between the applied field H and system width L for various fixed lifetimes (solid curves) in a typical metastable magnetic system. Four regions are distinguished by differing decay processes: the Coexistence region (CE), the Single-Droplet region (SD), the Multi-Droplet region (MD), and the Strong-Field region (SF). The CE and SD regions are separated by the thermodynamic spinodal (dotted curve). The SD and MD regions are separated by the dynamic spinodal (dash-dotted curve). The SF region is separated from the other regions by the mean-field spinodal (dashed curve).

FIG. 2. The relationship between the applied field H and system width L for various fixed lifetimes (solid curves) and temperatures as calculated through kinetic Ising model simulations. The thermodynamic spinodal (dotted curve) is calculated from Eq. (7). The mean-field spinodal is approximated by $H_{1/2}$ (dash-dotted curve), calculated from Eq. (12). The mean-field spinodal (calculated from Eq. (16)) is not shown, since for each of the three temperatures it occurs at a field much larger than the displayed range. a) $k_B T = 0.65J$. b) $k_B T = 1.30J$. c) $k_B T = 0.8k_B T_c \approx 1.81535J$. The estimate for the Dynamic Spinodal given by Eq. (23) is shown by the dot-dot-dashed curve.

FIG. 3. $P(m > 0)$ vs. the time t in MCSS for the kinetic Ising model at a temperature of $T = 0.8T_c$. Note the different time scales. (a) $L = 6$ and $H = 0J$, in the coexistence region. (b) $L = 20$ and $H = -0.105J$, in the single-droplet region. (c) $L = 100$ and $H = -0.34725J$, in the multi-droplet region. The solid curve is a fit to Eq. (19). (d) $L = 30$ and $H = -3.5J$, in the strong-field region.

FIG. 4. $P(m > 0)$ vs. the applied field H for a kinetic Ising system at a temperature of $T = 0.8T_c$. (a) $\tau = 4670$ MCSS and $L = 6$, in the coexistence region. The horizontal line is $(1 + e^{-2})/2$. (b) $\tau = 914$ MCSS and $L = 10$, in the single-droplet region. The solid curve is a least-squares fit of Eq. (18) to the MC data. The inset shows the fitted curve over a wider range of fields. (c) $\tau = 40.7$ MCSS and $L = 30, 100,$ and 300 , in the multi-droplet region. The solid curves are fits of Eq. (21) to the MC data. The dashed curve is the fit of Eq. (21) to the MC data for $L = 100$, with the width of the switching region reduced by a factor of $(300/100)^{-d/2}$ to compare with the MC data for $L = 300$. (d) $L = 30$ and $\tau = 0.8$ MCSS, in the strong-field region.

FIG. 5. Spin configurations showing the nucleation and growth of several droplets in a typical realization of magnetization switching in the MD region. Here $L = 120$, $H = -0.2J$, and $T = 0.8T_c$. The times shown are at a) $t = 50$ MCSS, b) $t = 114$ MCSS, and c) $t = 160$ MCSS. Grey squares are “up” spins and black squares are “down” spins.

TABLES

TABLE I. Constants used in Eqs. (19) and (21) to calculate the width of the switching region as a function of time and as a function of field, respectively. The derivation is given in the Appendix.

d	ψ_d
2	0.5628545
3	0.5109029

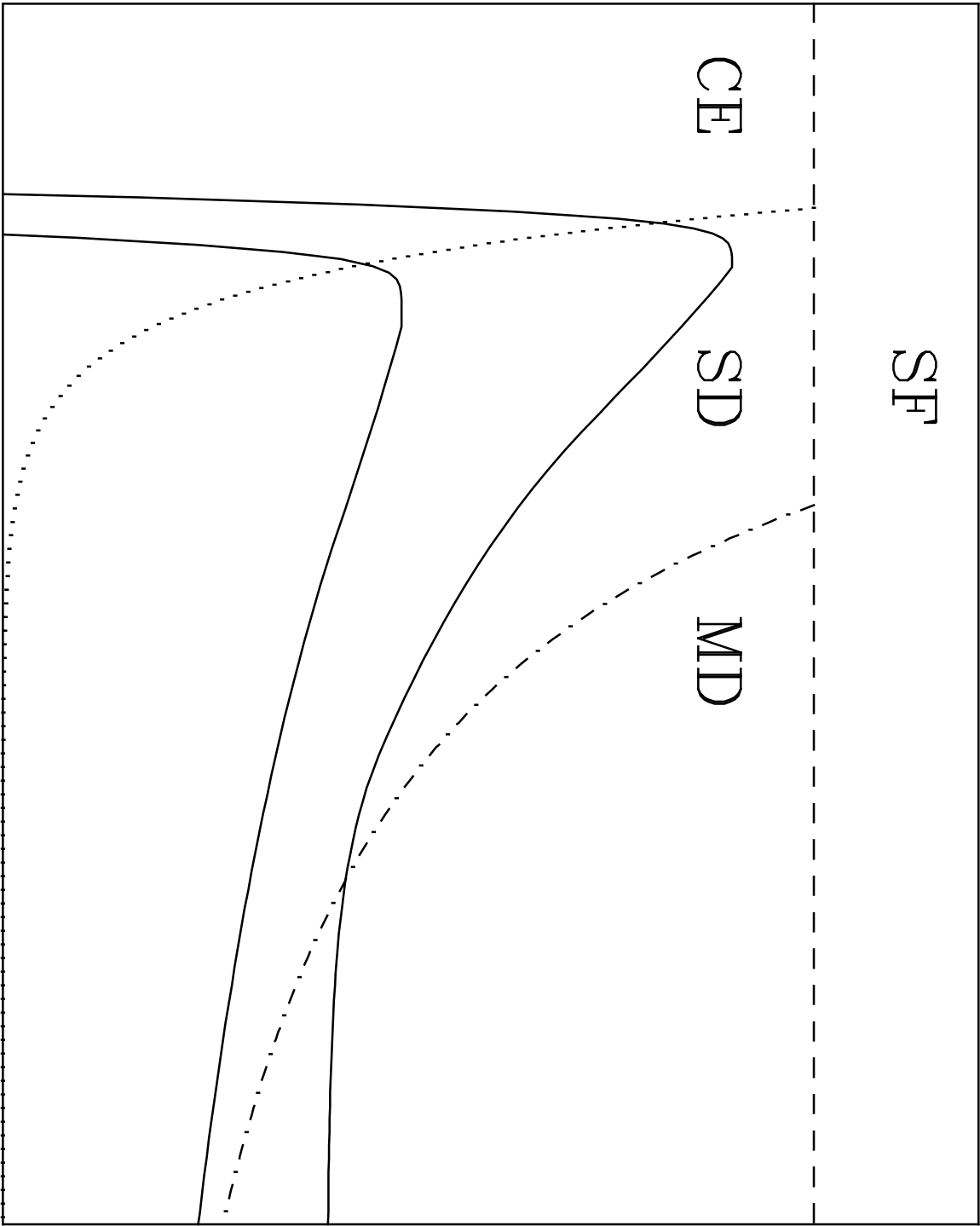
TABLE II. Results of fits of Eqs. (19) and (21) to MC data for $P(m > 0)$ at $T = 0.8T_c$. Estimated quantities are given with their statistical uncertainties.

L	Method	τ [MCSS]	$ H_{\text{sw}} /J$	νJ [1/MCSS]
30	P vs. H	40.7	0.34684(2)	0.96(1)
100	P vs. H	40.7	0.347253(2)	0.92(2)
100	P vs. t	40.8(4)	0.34725	0.97(1)

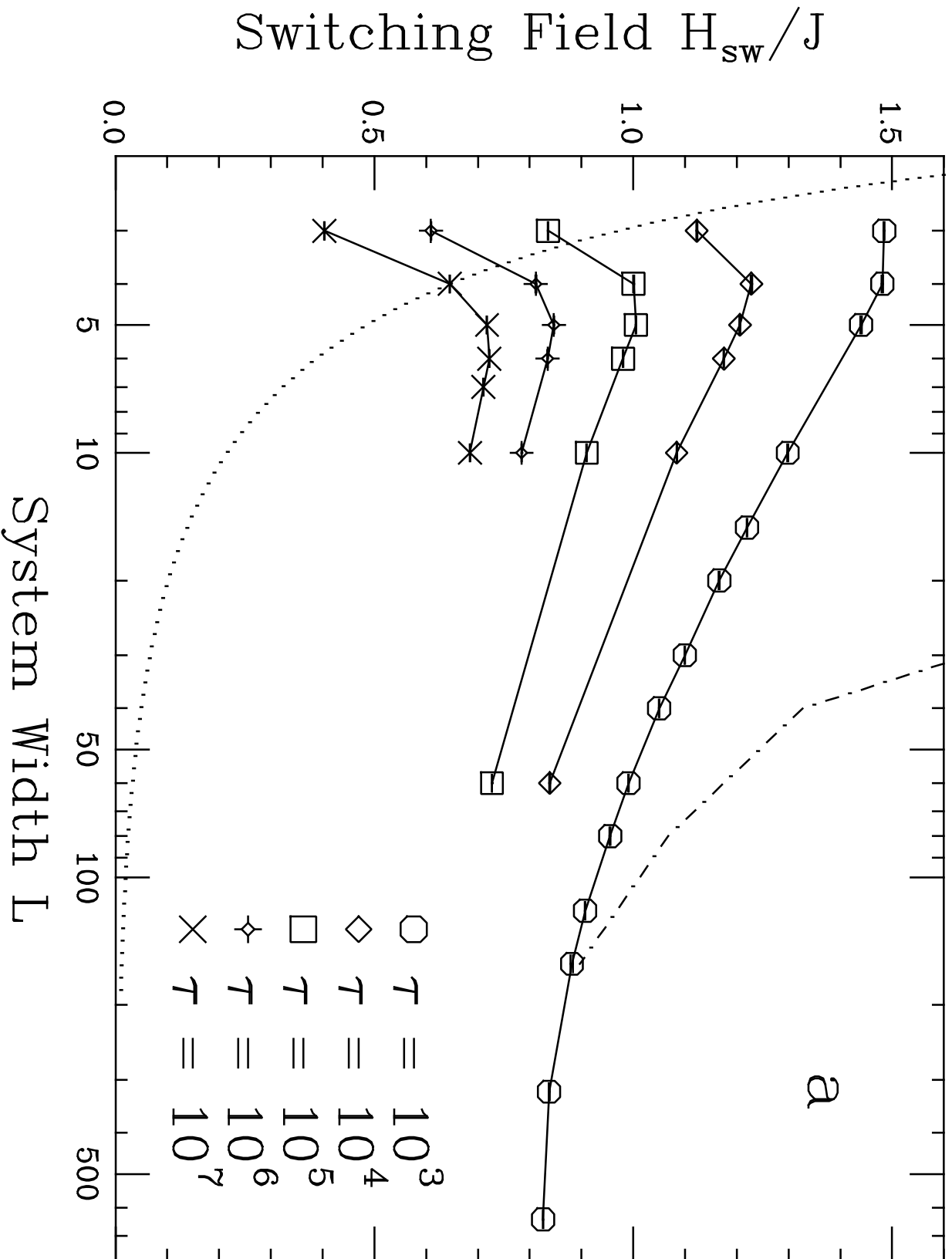
"MAGNETIZATION SWITCHING IN NANOSCALE ..." by RICHARDS, SIDES, NOVOTNY, RIKVOLD

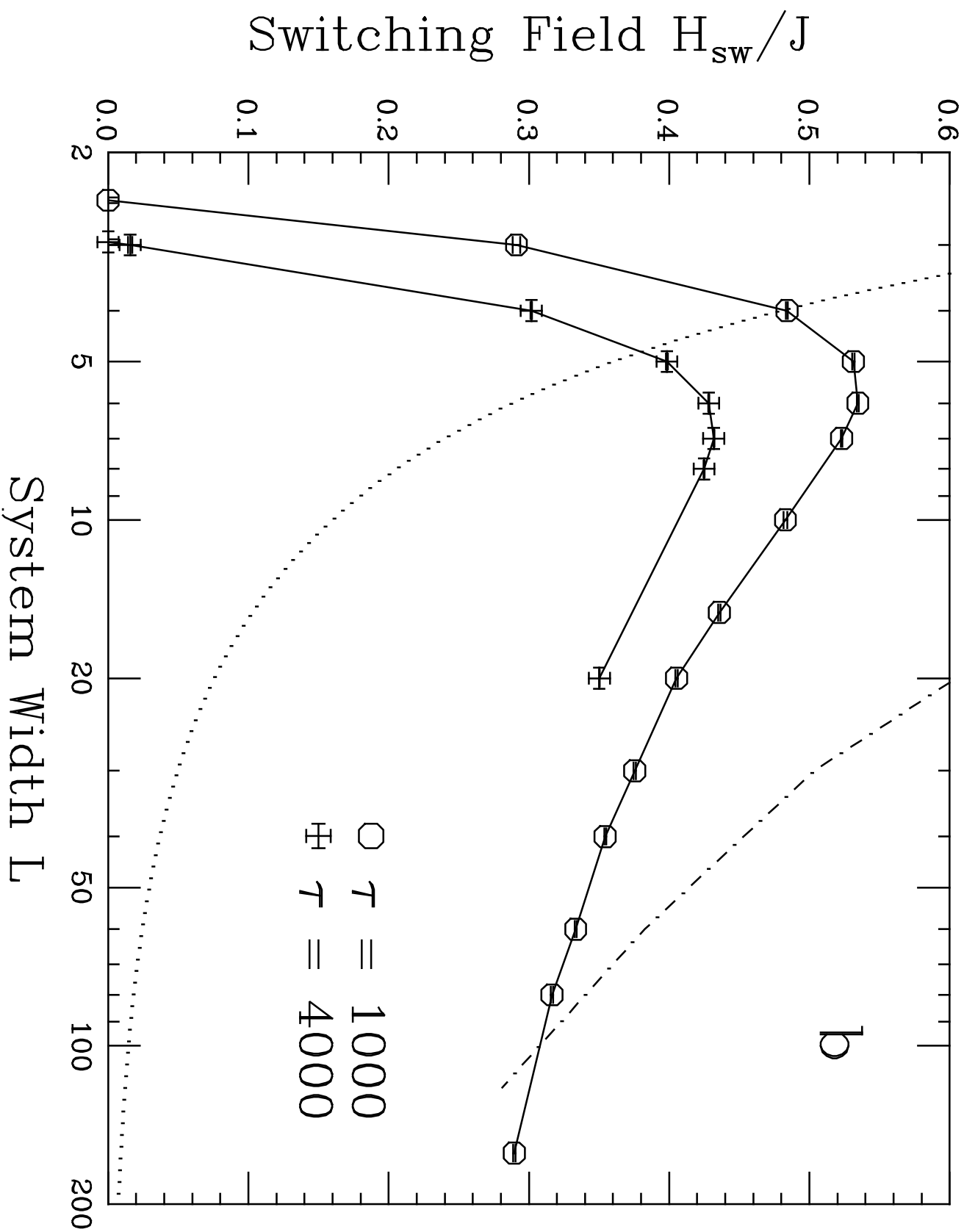
Fig. 1

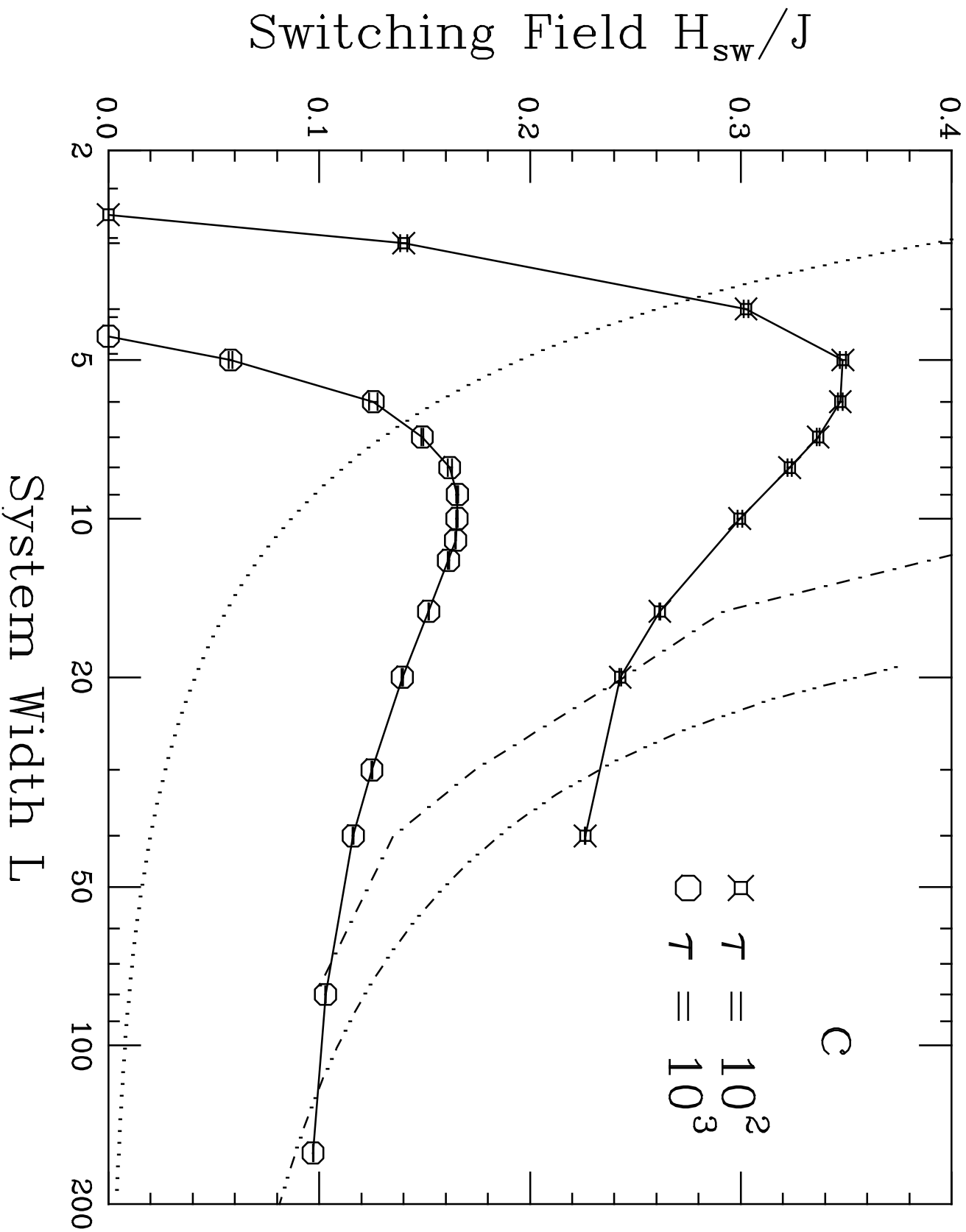
Switching Field H_{sw}



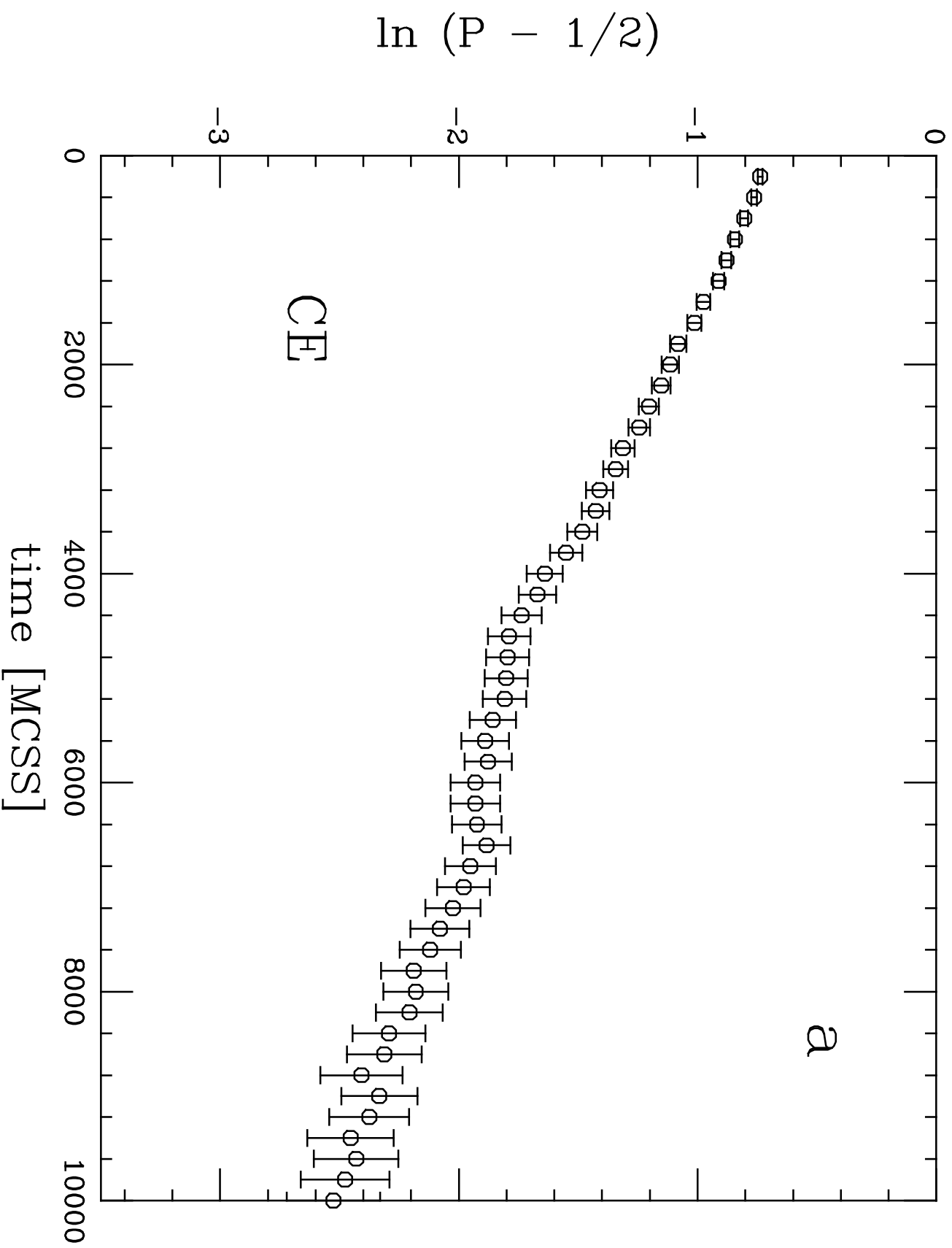
$\ln L$

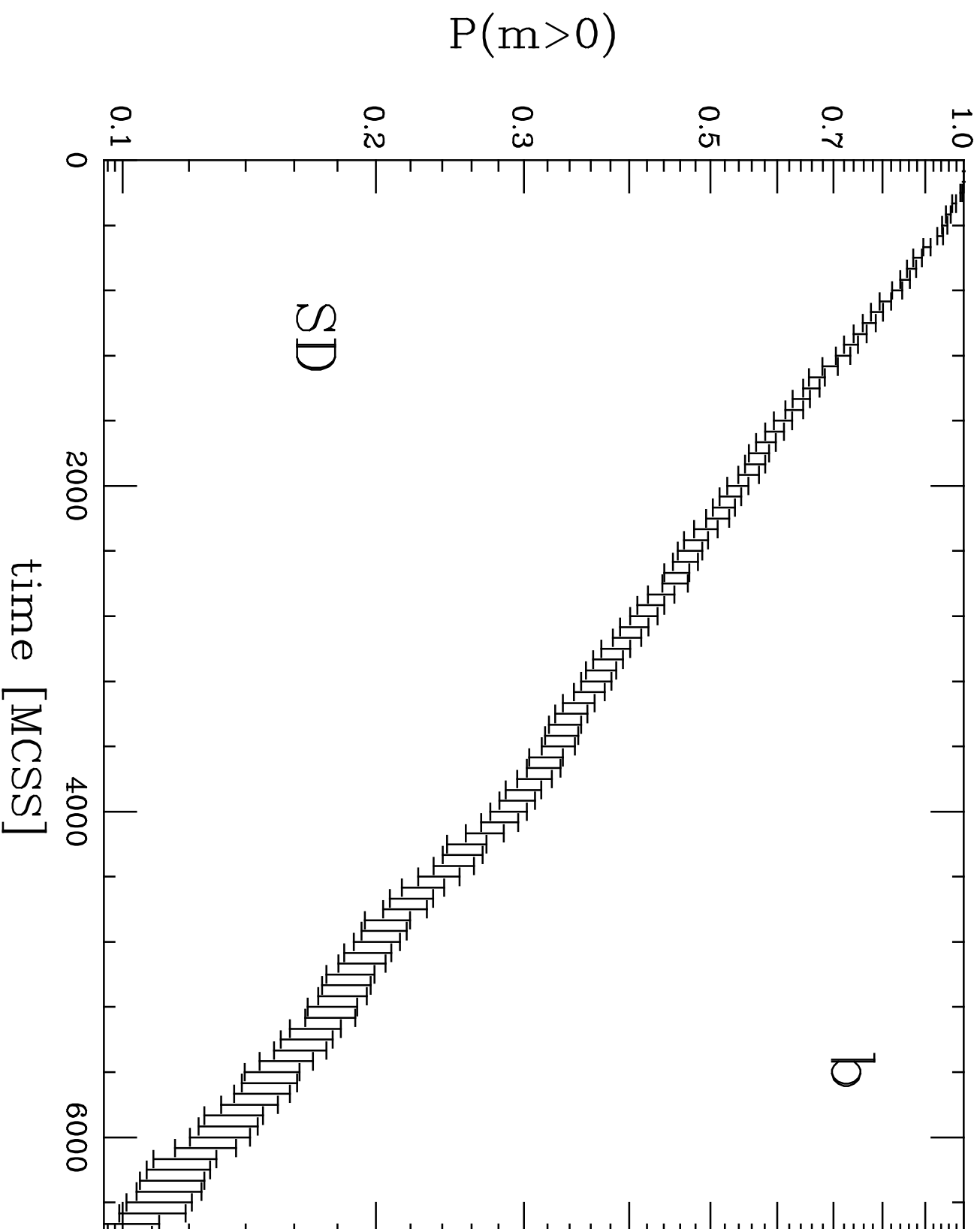




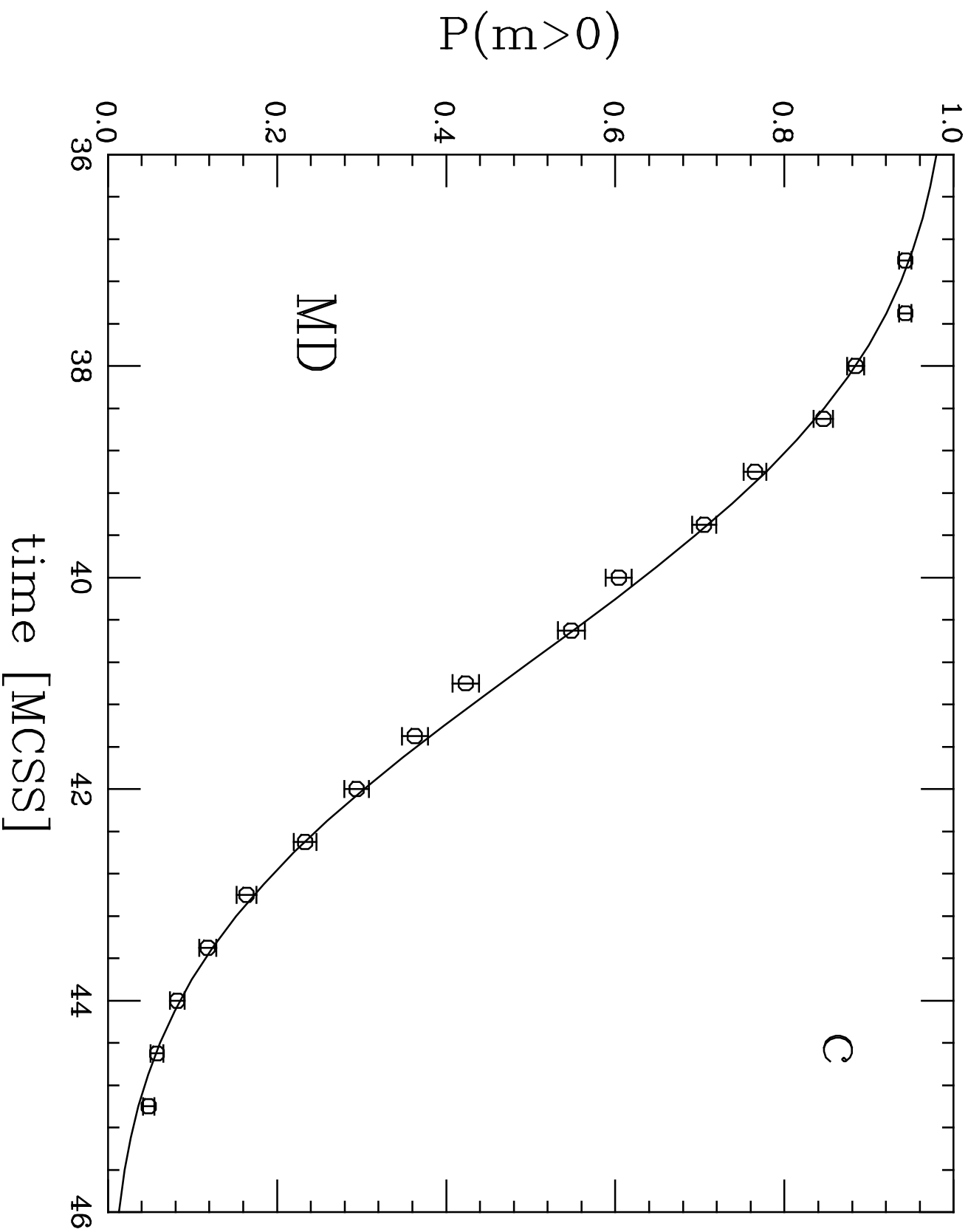


"MAGNETIZATION SWITCHING IN NANOSCALE ..." by RICHARDS, SIDES, NOVOTNY, RIKVOLD FIG. 3a

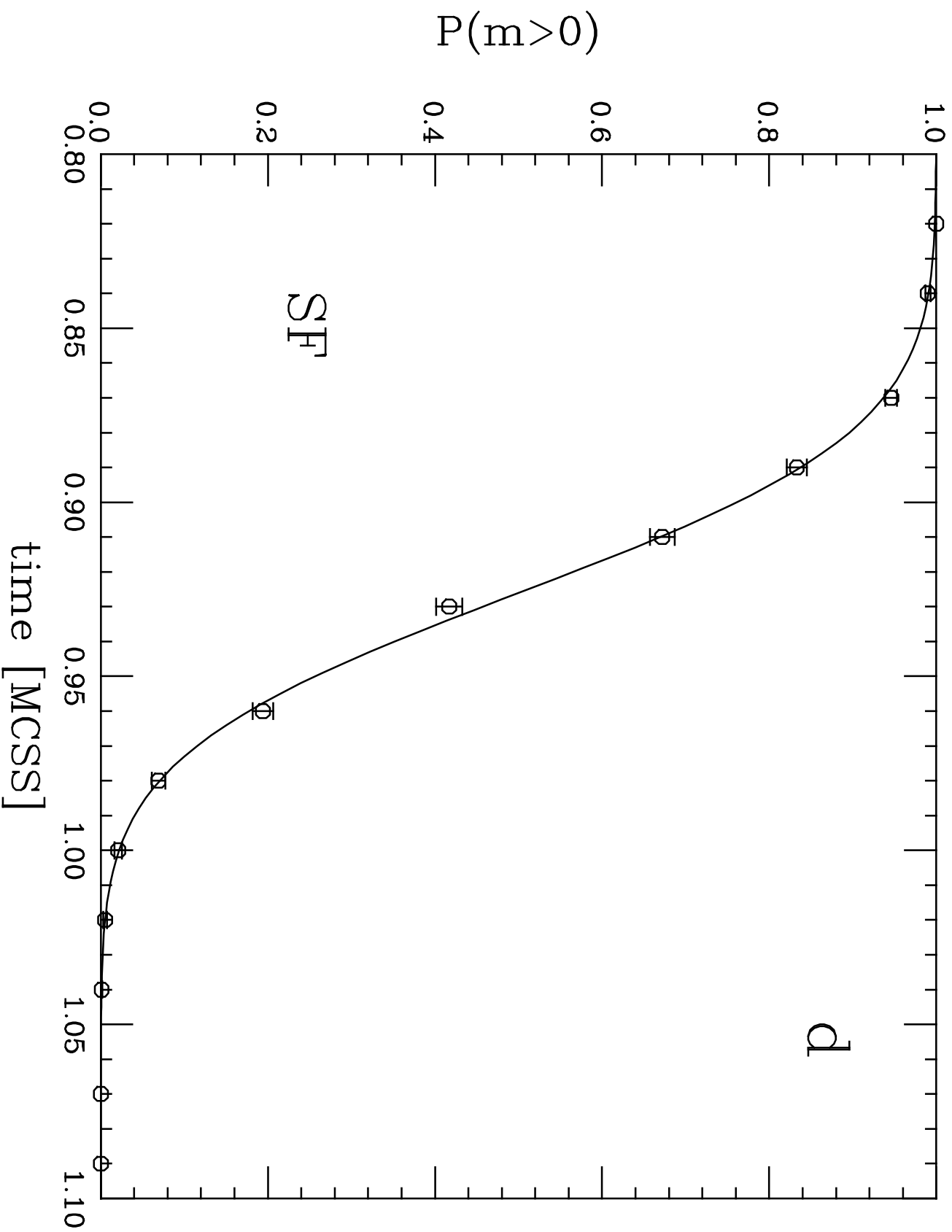


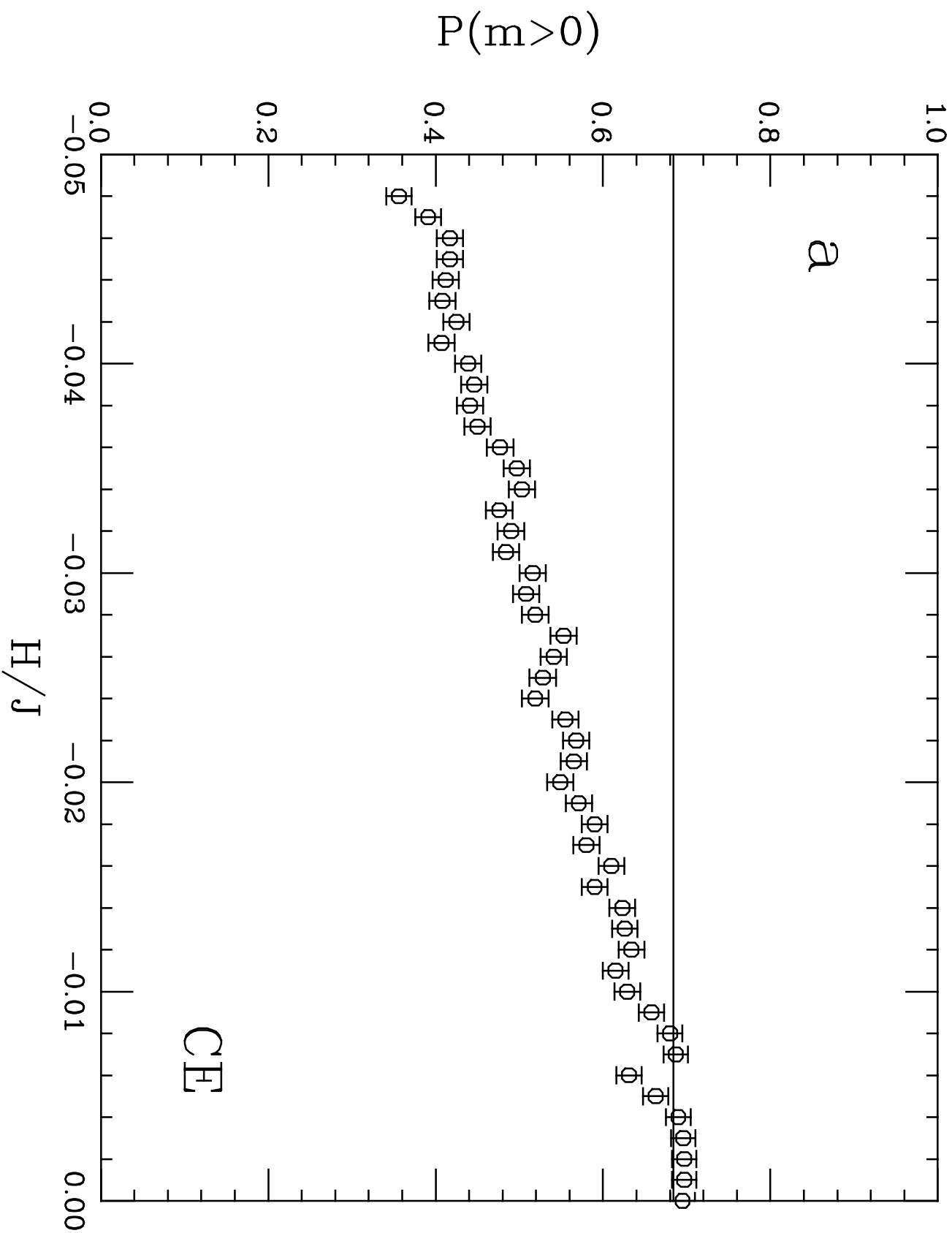


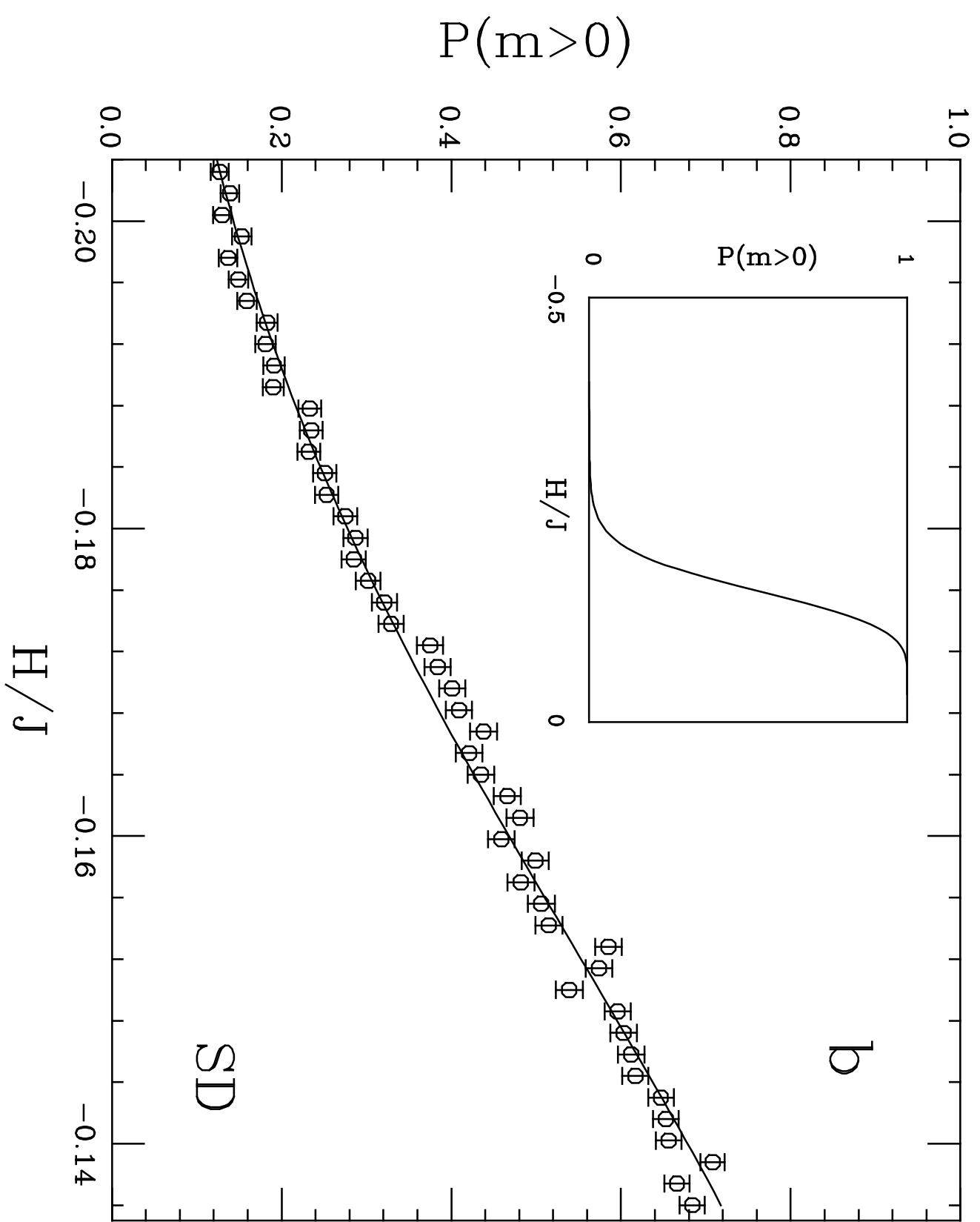
MAGNETIZATION SWITCHING IN NANOSCALE ... by RICHARDS, SIDES, NOVOTNY, RIKVOLD FIG. 3c



"MAGNETIZATION SWITCHING IN NANOSCALE ..." by RICHARDS, SIDES, NOVOTNY, RIKVOLD FIG. 3d







"MAGNETIZATION SWITCHING IN NANOSCALE ..." by RICHARDS, SIDES, NOVOTNY, RIKVOLD FIG. 4C

